agronomy

MDPI

Article

The Efficacy of Sunn Hemp (*Crotalaria juncea*) and Fe_3O_4 Nanoparticles in Controlling Weed Seed Germination

Fatemeh Ahmadnia [1], Ali Ebadi [1], Mohammad Taghi Alebrahim [1], Ghasem Parmoon [2], Solmaz Feizpoor [3] and Masoud Hashemi [4,*]

[1] Department of Plant Production and Genetics, Faculty of Agricultural Sciences & Natural Resources, University of Mohaghegh Ardabili, Ardabil 56199-11367, Iran; f.ahmadnia@uma.ac.ir (F.A.)
[2] Sugar Beet Research Department, Kermanshah Agricultural and Natural Resources Research and Education Center, Education and Extension Organization (AREEO), Kermanshah 14968-13111, Iran
[3] Wuhan National Laboratory for Optoelectronics, School of Integrated Circuits, Huazhong University of Science and Technology, Wuhan 430074, China
[4] Stockbridge School of Agriculture, University of Massachusetts, Amherst, MA 01003, USA
* Correspondence: masoud@umass.edu

Abstract: Utilizing nanotechnology for weed management offers a sustainable alternative to synthetic herbicides. This study evaluated the effectiveness of sunn hemp extract (SH), Fe_3O_4 nanoparticles (NPs), and Fe_3O_4/sunn hemp NPs in inhibiting the germination of redroot pigweed (*Amaranthus retroflexus* L.), wild mustard (*Sinapis arvensis* L.), and lamb's quarters (*Chenopodium album* L.) weeds. The structural characteristics of the NPs were analyzed using Scanning electron microscopy (SEM), Scanning X-ray diffraction (XRD), Thermogravimetric analysis (TGA), Vibrating sample magnetometer (VSM), Brunner–Emmet–Teller (BET), and Fourier-transform infrared spectroscopy (FTIR). The optimal Fe_3O_4 NP concentration for reducing seed germination ranged from 3000 to 3100 mg L^{-1}. Higher concentrations of SH extract (100, 150, and 200 g L^{-1}) effectively inhibited weed seed germination with *A. retroflexus* displaying the highest sensitivity. The maximal effective concentration ($NOEC_{max}$) for Fe_3O_4/sunn hemp NPs was 10 g L^{-1} for *S. arvensis*, 150 g L^{-1} for *A. retroflexus*, and 200 g L^{-1} for *C. album*. Fe_3O_4/sunn hemp NPs led to a reduction in $1/D_{50}$ and an increase in EEC_{50}, indicating a rise in sensitivity to Fe_3O_4 NPs, particularly in *S. arvensis*. Variations in species responses to SH, Fe_3O_4 NPs, and Fe_3O_4/sunn hemp NPs are likely influenced by genetic, physiological, and ecological factors. Overall, the findings suggest that utilizing Fe_3O_4/sunn hemp NPs offers an effective strategy for sustainable weed management.

Keywords: Fe_3O_4 nanoparticles; sunn hemp allelopathy; *Amaranthus retroflexus*; *Sinapis arvensis*; *Chenopodium album*

Academic Editor: Rosana Marta Kolb

Received: 12 February 2025
Revised: 20 March 2025
Accepted: 21 March 2025
Published: 24 March 2025

Citation: Ahmadnia, F.; Ebadi, A.; Alebrahim, M.T.; Parmoon, G.; Feizpoor, S.; Hashemi, M. The Efficacy of Sunn Hemp (*Crotalaria juncea*) and Fe_3O_4 Nanoparticles in Controlling Weed Seed Germination. *Agronomy* **2025**, *15*, 795. https://doi.org/10.3390/agronomy15040795

1. Introduction

Competition with weeds poses a significant biological challenge to crop production, contributing up to a 34% reduction in crop yields [1,2]. While the use of relatively low-cost synthetic chemicals for weed control offers short-term effectiveness and ease of application, there is an increasing need for farming practices that offer more sustainable and environmentally friendly strategies [3–7].

Nanotechnology has emerged as an alternative weed control [8,9]. Nanoparticles (NPs), typically less than 100 nm in size, exhibit unique electrochemical, optical, and thermal properties. Nevertheless, the synthesis of metallic NPs may pose environmental hazards attributable to the application of highly reactive and toxic reducing agents,

including sodium borohydride and hydrazine hydrate [10]. To mitigate these concerns, green chemistry methods have been proposed to produce more environmentally friendly NPs, using extracts from plants such as barley (*Hordeum vulgare*) and sorrel (*Rumex acetosa*) [11] and methanolic extracts from grape leaves [12] to stabilize Fe_3O_4 NPs. These processes highlight the role of biomolecules, such as phytols, terpenoids, and antioxidants in synthesizing Fe_3O_4 NPs.

Sunn hemp, a C_3 tropical crop from Fabaceae family, is known for its resilience to harsh environmental conditions and traditionally is used as a cover crop for nitrogen biological fixation [13]. It offers various ecosystem benefits, including suppression of weeds [14], parasitic nematodes [15], in addition to the improvements in soil health [16]. Sunn hemp's ability to produce substantial biomass contributes to its effectiveness in weed suppression [17], but also releases allelopathic compounds such as hydroxy norleucine, a phytotoxic non-protein amino acid, from its decomposing residues [18]. Sunn hemp seeds also contain 2-amino-5-hydroxyhexanoic acid, another amino acid with weed-suppressing properties [19]. Furthermore, sunn hemp's root, stem, and seeds contain dehydropyrrolizidine alkaloids, which contribute to weed suppression abilities [20]. These alkaloids are found in varying concentrations in different plant parts, including 0.150% *w*/*w* in seeds, 0.115% *w*/*w* in stems, 0.053% *w*/*w* in roots, and 0.008% *w*/*w* in leaves [21]. Alkaloids such as riddelliine, senecionine, and seneciphylline are known for their allelopathic effects in weed suppression [19]. However, concerns have been raised about relying solely on the allelopathic effect of cover crops for weed management due to the negligible amounts of allelopathic compounds in the plants. Combining allelopathic compounds from plant extracts with NPs may present a novel approach to integrated weed management.

Redroot pigweed (*Amaranthus retroflexus*), lamb's quarters (*Chenopodium album*), and wild mustard (*Sinapis arvensis*) are amongst most common weeds in many agricultural fields. These species hinder crop growth and reduce yield due to their rapid growth, prolific seed production, and ability to germinate under diverse environmental conditions. Several studies have explored the effects of aqueous and methanolic extracts, as well as essential oils derived from allelopathic plants, on the germination of these invasive weed species [22–24]. The application of sunn hemp leaf extract significantly reduced germination in various crops, including Poaceae (cereal rye, sweet corn, winter wheat 2–22%), Solanaceae (tomato, bell pepper 100%), Fabaceae (Austrian winter pea, cowpea, crimson clover 39–8%), Liliaceae (onion 95%), Brassicaceae (turnip 69%), Malvaceae (okra 49%), and Cucurbitaceae (cucumber 2%) [25].

In this study, we hypothesized that an aqueous extract derived from sunn hemp leaves can significantly prevent the germination of weed species. Previous research has shown that natural extracts that possess phytotoxic properties can make them viable alternatives to synthetic herbicides. We propose that green synthesis of Fe_3O_4 NPs using sunn hemp leaf extract may further enhance the inhibition of germination, surpassing the effects of the extract alone. This investigation aims to evaluate the effectiveness of the sunn hemp aqueous extract, Fe_3O_4 NPs, and the synthesized Fe_3O_4/sunn hemp NPs in controlling the germination of the three common weed species. We seek to determine whether the combination of NPs and plant extracts offers a more effective approach to weed management. This research therefore may contribute to the sustainability of farming by providing an eco-friendly alternative to synthetic herbicides and promoting an environmentally sustainable approach to managing weed growth.

2. Materials and Methods

2.1. Sunn Hemp Biomass and Extract Preparation

Sunn hemp (*Crotalaria Juncea* L.), (Global Sunn brand) was grown in the field at the Experimental Research Station of the Department of Plant Production and Genetics, University of Mohaghegh Ardabili, Iran, with geographical coordinates 48°20′ E, 38°19′ N in 2022. Sunn hemp was planted at the recommended seeding rate, 50 kg ha^{-1} [26]. The leaves of the plants at the onset of the blooming phase, approximately 65 days after planting, were harvested by hand [25]. The collected material was completely dried at room temperature (23 ± 2 °C) for 30 days because phenolics are not stable for drying in an oven at high temperatures [27]. The extract was prepared utilizing the maceration technique outlined by Trusheva et al. [28]. In brief, specified amounts of sunn hemp powder (0, 10, 50, 100, 150, and 200 g L^{-1}) were added to one liter of distilled water, and placed on the shaker for 24 h. The solution was filtered through Whatman No. 42 filter paper and centrifuged for 15 min at 5000 rpm to remove the solids. The separated supernatant, referred to hereafter as the sunn hemp extract, was kept in the refrigerator at 4 °C until germination tests were conducted.

2.2. Seed Gathering and Storage

The experiment aimed to study the impact of the aqueous extract of sunn hemp, Fe_3O_4 NPs, and Fe_3O_4/sunn hemp NPs on the germination of the three weed species lamb's quarters (*Chenopodium album* L.), redroot pigweed (*Amaranthus retroflexus* L.), and wild mustard (*Sinapis arvensis* L.). The weed seeds were collected from fields in Moghan Research and Natural Resources Center located at 48°20′ E, 38°19′ N during the summer of 2022. Weed-ripening inflorescences were gathered and air-dried at 23 ± 2 °C for three weeks, after which seeds were separated by rubbing. Germination tests on freshly harvested seed showed that *C. album*, *A. retroflexus*, and *S. arvensis* had high primary dormancy. We broke the primary seed dormancy by treating them with ultrasound technology and gibberellic acid at 15 min and 1500, and 1000 mg L^{-1}, respectively [29–31]. The weed seeds were stored in a dry environment at room temperature (23 ± 2 °C) for four days before the experiment started.

2.3. Biosynthesis of Fe_3O_4 NPs

The Fe_3O_4 NPs were synthesized through the co-precipitation technique described by Massart, [32]. Initially, water was degassed by blowing N_2 gas for 20 min. For the synthesis, 0.476 g of $FeCl_3 \cdot 6H_2O$ was dissolved in 20 mL of the degassed water (Solution A). In a separate preparation, 0.166 g of $FeCl_2 \cdot 4H_2O$ was added to 5 mL of degassed water and 0.8 mL of 2 M HCl (Solution B). Solutions A and B were combined with 13.1 mL of NH_3 and 20 mL of sunn hemp extract, while N_2 gas was continuously blown into the solutions. After stirring for 60 min, the brown precipitate was refluxed for an additional hour to ensure a complete reaction. The resulting precipitate was then washed with water and ethanol before drying. Additionally, pure Fe_3O_4 NPs was synthesized using the same method, omitting the sunn hemp extract (Scheme 1, Reaction Equation (1)).

$$Fe^{2+} + 2Fe^{3+} + OH^- \rightarrow Fe(OH)_2 + 2Fe(OH)_3 \xrightarrow[-H_2O]{\Delta} Fe_3O_4 \quad (1)$$

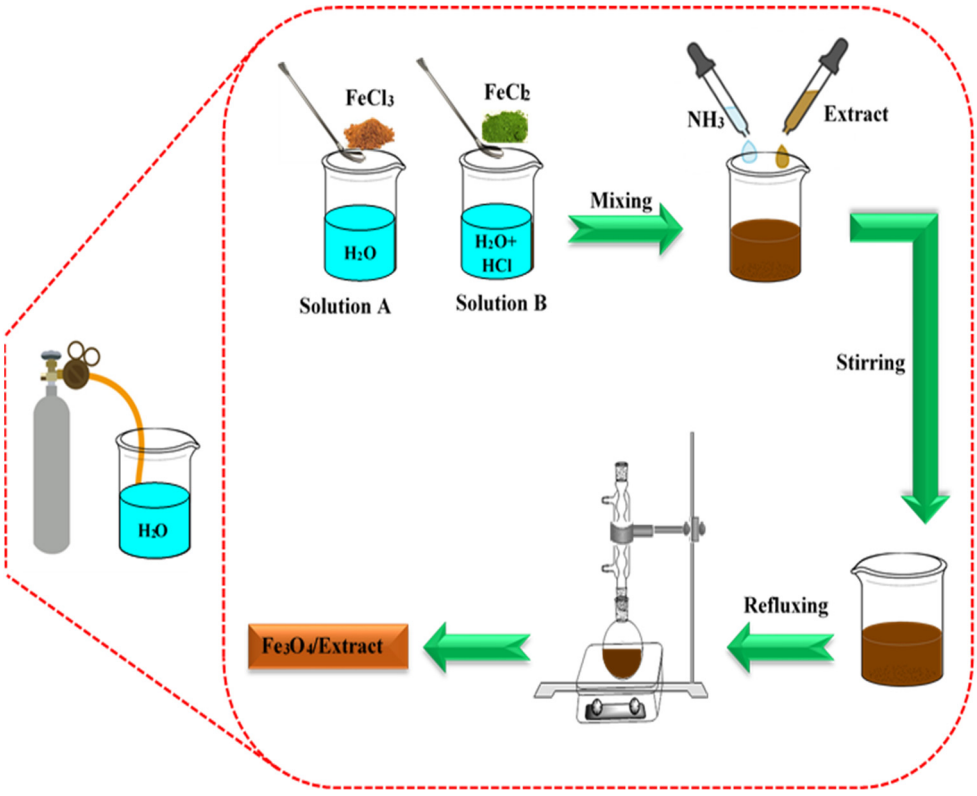

Scheme 1. Schematic of Fe_3O_4/sunn hemp extract synthesis.

2.4. Characterization Techniques

Thermogravimetric analysis (TGA, LINSEIS STA PT-1000, LINSEIS Messgeräte GmbH, Selb, Germany) and vibrating sample magnetometer (VSM, MDKF, Magnetic Daneshpajoh Kashan (MDK) Co., Kashan, Iran), Fourier-transform infrared spectroscopy (FTIR, Perkin Elmer Spectrum RXI, PerkinElmer Co., Hopkinton, MA, USA), Scanning electron microscope (SEM, LEO 1430VP, LEO Electron Microscopy Ltd., Cambridge, UK and Carl Zeiss AG, Jena, Germany), X-ray diffraction (XRD, Philips Xpert diffractometer, Philips Co., Eindhoven, The Netherlands), and Brunner–Emmet–Teller (BET, Belsorp Mini II, MicrotracBEL Corp., Osaka, Japan) analysis were employed to assess the thermal and magnetic properties, analyze the chemical structure and functional groups, investigate the microstructures and crystal structure of the nanomaterials, and evaluate their textural characteristics.

2.5. Experimental Design

The study was executed in 2022 at the Weed Science Laboratory, Faculty of Agriculture and Natural Resources at Mohaghegh Ardabili University. The bioassay experiments were conducted in two parts. In the first part, the focus was on optimizing the impact of Fe_3O_4 NPs on the germination of seeds. A germination test was carried out using different concentrations of Fe_3O_4 NPs (0, 250, 500, 1000, 2000, and 3000 mg L^{-1}) to determine the half-maximal effective concentration ($NOEC_{50}$) and maximal effective concentration ($NOEC_{max}$) within two defined ranges. Subsequently, Fe_3O_4 NPs containing sunn hemp extract were synthesized using green methods. In the second part, a germination test was performed using 0, 10, 50, 100, 150, and 200 g L^{-1} (or 0, 1, 5, 10, 15, and 20%) of pure sunn hemp extract and Fe_3O_4/sunn hemp NPs in three points (SH (Sunn hemp extract), SH + $NOEC_{50}$, and SH + $NOEC_{max}$). Both parts of the experiment were conducted using a completely randomized design with three replications for each weed seed. Each Petri dish contained 50 seeds disinfected with 1% sodium hypochlorite placed on filter paper within 9 mm diameter Petri dishes. Ten milliliters of the treatments (SH extract, Fe_3O_4 NPs,

and Fe_3O_4/sunn hemp NPs) were added to each Petri dish, which was then covered with transparent plastic wrap and transferred to a seed germinator (BINDER KBW 240, Binder GmbH, Tuttlingen, Deutschland, Germany) set at a temperature of 25 °C without light. Germination experiments lasted 14 days. Seeds exhibiting healthy radicles that reached a length of two millimeters were classified as successfully germinated [33].

2.6. Gas Chromatography–Mass Spectrometry (GC-MS)

The analytical procedures utilized an Agilent 7890B Gas Chromatography system paired with an Agilent 5977A Mass Selective Detector (MSD), Agilent Technologies Inc, Palo Alto, CA, USA. A sample injection volume of 0.1 µL was used, with helium gas serving as the carrier. The multimode inlet (MMI) operated in split mode with a 15:1 ratio and a flow rate of 48 mL/min. The MMI's initial temperature started at 100 °C and was raised to 380 °C at 8 °C/min, while the oven began at 40 °C and increased to 325 °C at 4 °C/min before rising to 400 °C at 10 °C/min, held for 12.5 min. The total analytical duration was 91.25 min.

2.7. Statistical Analysis

Cumulative germination percentage: The cumulative germination percentage represents the overall count of seeds that successfully sprouted within the experimental sample.

Final germination percentage (G_{max}): Scott et al.'s [34]. and Burnett et al.'s [35] Equation (2) was used to calculate the G_{max}.

$$G_{max} = \frac{S}{T} \times 100 \tag{2}$$

where S indicates the number of germinated seeds, and T refers to the total number of seeds included in the sample.

For the determination of the regression trend of parameters, we used the non-linear regression function of Logistic (Equation (3)) and Comperze (Equation (4)) using R 2.4.1 software.

$$Y = \frac{Y_{max}}{1 + \left(-\left(\frac{x}{EC_{50}}\right)\right)^{slope}} \tag{3}$$

$$Y = Y_{max} \times \exp\left(-\exp\left(\frac{-(x - EC50)}{slope}\right)\right) \tag{4}$$

where Y_{max} represents the maximum value of y, and EC_{50} denotes the half-maximal effective concentration. The parameters' best estimates were assessed using R^2 (coefficient of determination) and RMSE (root mean square error), which were computed using Equations (5) and (6), respectively.

$$R^2 = \frac{SSR}{SST} \tag{5}$$

$$RMSE = \sqrt{\frac{\sum_{i=1}^{N}(Ypred - Yobs)^2}{N}} \tag{6}$$

where SSR denotes the sum of squares due to regression, and SST represents the total sum of squares. Yobs refers to the observed value, Ypred indicates the predicted value, and n signifies the number of samples.

3. Results

3.1. Characterization of Prepared NPs

The XRD analysis was executed to assay the purity and crystallinity of the Fe_3O_4 NPs and Fe_3O_4/sunn hemp NPs (20%) samples, as demonstrated in Figure 1a. The diffraction

patterns of both Fe_3O_4 NPs and Fe_3O_4/sunn hemp NPs (20%) revealed peaks corresponding to the (220), (311), (400), (422), (511), and (440) planes, positioned at 2θ values of 30.1°, 35.5°, 43.3°, 53.5°, 57.1°, and 62.8°, respectively [36]. No alterations in the crystal structure of Fe_3O_4 NPs were detected following the addition of the extract. The distinct diffraction peaks of samples were consistent with cubic inverse spinel structures (JCPDS file No. 01–075–0033) [37,38]. Furthermore, the absence of impurity peaks in the XRD patterns suggests that the synthesized NPs are of high purity.

The SEM images provided insights into the microstructures of the Fe_3O_4 NPs, Fe_3O_4/sunn hemp NPs (15%), and Fe_3O_4/sunn hemp NPs (20%) samples, showing that Fe_3O_4 NPs and Fe_3O_4/sunn hemp NPs samples possessed nearly spherical shapes (Figure 1b–d) [39].

FTIR analysis was performed to detect the functional groups present in the Fe_3O_4 NPs, Fe_3O_4/sunn hemp NPs (15%), and Fe_3O_4/sunn hemp NPs (20%) nanomaterials, as shown in Figure 1e. The absorbance bands for O-H stretching and bending vibrations were identified at 3200–3500 cm^{-1} and 1662 cm^{-1}, respectively [40,41]. The bands ranging from 579 to 632 cm^{-1} corresponded to the stretching vibration of Fe-O [42]. The characteristic peaks of C-O stretching, and C-H stretching were found around 1120 and 1440 cm^{-1}, respectively [43,44].

Thermal stability of the Fe_3O_4 NPs and Fe_3O_4/sunn hemp NPs (20%) was assessed through TGA, revealing minimal weight loss below 200 °C attributed to the evaporation of adsorbed water from the samples. The maximum weight loss of samples occurred between 250 and 700 °C, due to the decomposition of organic compounds surrounding the samples (Figure 1f).

BET analysis was used to assess the textural characteristics of the Fe_3O_4 NPs, Fe_3O_4/sunn hemp NPs (15%), and Fe_3O_4/sunn hemp NPs (20%) samples. The N_2 adsorption–desorption isotherms of the samples are displayed in Figure 1g, revealing a type II nitrogen isotherm characteristic of mesoporous structures for all the samples. Pure Fe_3O_4 NPs had the largest surface area followed by Fe_3O_4/sunn hemp NPs samples, with values of 35.8, 10.7, and 6.2 m^2g^{-1}, for the Fe_3O_4 NPs, Fe_3O_4/sunn hemp NPs (15%), and Fe_3O_4/sunn hemp NPs (20%) samples, respectively. Table 1 demonstrates the details of porosity measurement information.

Table 1. Textural properties of the prepared sunn hemp samples.

Sample	Surface Area (m^2g^{-1})	Mean Pore Diameter (nm)	Total Pore Volume (cm^3g^{-1})
Fe_3O_4	35.8	4.677	0.041
Fe_3O_4/Extract (15%)	10.7	4.006	0.010
Fe_3O_4/Extract (20%)	6.2	3.703	0.005

Fe_3O_4/sunn hemp (15%), Fe_3O_4/sunn hemp 150 g L^{-1}; Fe_3O_4/sunn hemp (20%), Fe_3O_4/sunn hemp 200 g L^{-1}.

To explore the magnetic characteristics of the nanomaterials, VSM analysis was performed. Figure 1h reveals the magnetization curves of Fe_3O_4 NPs, Fe_3O_4/sunn hemp NPs (15%), and Fe_3O_4/sunn hemp NPs (20%) with a magnetic field of −12,000 to 12,000 Oe at 300 K. The saturation magnetization (Ms) of 17.05 $emug^{-1}$ was obtained for Fe_3O_4 NPs, while the Ms value reduced to 12.71 and 11.27 $emug^{-1}$ for Fe_3O_4/sunn hemp NPs (15%) and Fe_3O_4/sunn hemp NPs (20%) samples, respectively. With the incorporation of a non-magnetic extract to the surface of Fe_3O_4 NPs, the Ms value of the Fe_3O_4/sunn hemp NPs samples was reduced when compared with the Fe_3O_4 NPs. Nevertheless, the magnetic properties of the Fe_3O_4/sunn hemp NPs samples were sufficient to allow separation from the solution using an external magnetic field.

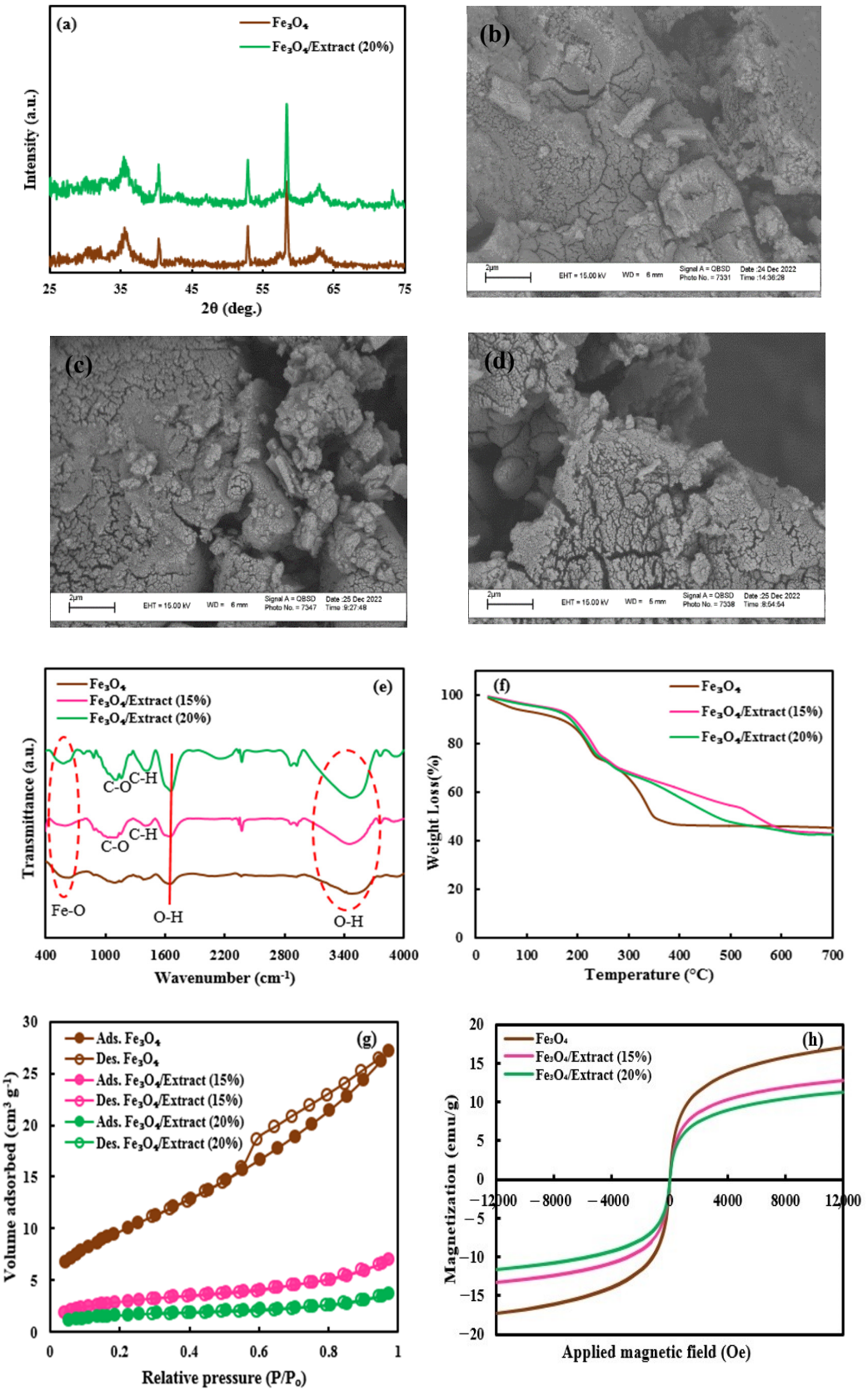

Figure 1. XRD (**a**), SEM images (**b**–**d**), FTIR (**e**), TGA (**f**), BET (**g**), and VSM (**h**) analyses of the prepared nanomaterials. Fe_3O_4, Pure Fe_3O_4; Fe_3O_4/Extract (15 and 20%), Fe_3O_4/sunn hemp (150 and 200 g L^{-1}) NPs.

3.2. Optimizing the Fe_3O_4 NPs

Figure 2 displays the logistic function's optimized output for various concentrations of Fe_3O_4 NPs and indicates that the model fits the data well (RMSE = 3.10–6.09 and R^2 = 0.846–0.999). The final germination percentage (G_{max}) of three weed species was evaluated, and the use of Fe_3O_4 NPs up to 200 mg L^{-1} had no significant effect on weed seed germination. For example, the G_{max} in *A. retroflexus* in 0 and 200 mg L^{-1} of Fe_3O_4 NPs was about 100% and 80%, respectively. The G_{max} of *S. arvensis* and *C. album* in similar ranges from 100 to 80% and 77 to 68%, respectively. Furthermore, the $NOEC_{50}$ of Fe_3O_4 NPs, was obtained in concentrations between 765 and 980 mg L^{-1}, depending on the species. The *A. retroflexus* and *C. album* had the highest and lowest $NOEC_{50}$, respectively. The $NOEC_{max}$ was recorded at about 3000–3100 mg L^{-1} and weed species were not statistically different (Figure 2).

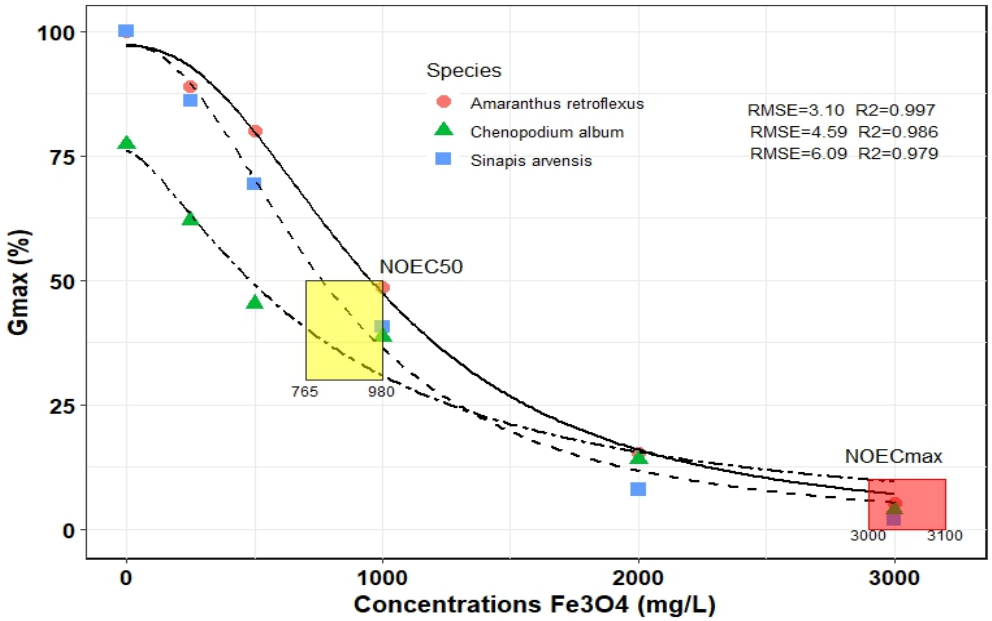

Figure 2. Final germination (G_{max}) of three weed species influenced by different concentrations of Fe_3O_4 NPs by fitted logistic model. The points correspond to the observed values, whereas the lines represent the predicted values. $NOEC_{50}$, half maximal effective concentration of Fe_3O_4 NPs; $NOEC_{max}$, maximal effective concentration of Fe_3O_4 NPs.

3.3. Effect of Fe_3O_4/Sunn Hemp NPs on Cumulative Germination

The Comperze model successfully fitted cumulative germination to investigate the germination initiation process of all three weed species, where R^2 ranged from 0.859 to 0.999 for *A. retroflexus*, 0.934 to 0.999 for *S. arvensis*, and 0.893 to 0.999 for *C. album* (Tables A1–A3 (Appendix A)). The estimated parameters indicated that *A. retroflexus* and *S. arvensis* reached their G_{max} (estimated by the model) of approximately 100%, while *C. album* reached its peak germination rate of 77% under normal conditions (distilled water) (Figure 3).

The use of SH extract resulted in a reduction of G_{max} and an increase in D_{50} (time to reach 50% germination); thus, the germination rate ($1/D_{50}$) of all weed species slowed down. For instance, when 50 g L^{-1} of SH was applied in the absence of Fe_3O_4 NPs, the G_{max} dropped by 85, 93, and 17 units in *A. retroflexus*, *S. arvensis*, and *C. album*, respectively. The results indicate that the use of Fe_3O_4 NPs at the optimized values for $NOEC_{50}$ and $NOEC_{max}$ alleviated the toxic effects of SH extract. For example, in the absence of Fe_3O_4 NPs, the application of 100 g L^{-1} of SH extract in *A. retroflexus* and *C. album* and 150 g L^{-1} in *S. arvensis* inhibited their G_{max}. However, in the presence of SH + $NOEC_{50}$

and SH + $NOEC_{max}$ of Fe_3O_4 NPs, the germination inhibition occurred at the presence of 150 and 200 g L^{-1} of SH extract, respectively. The results indicated that the *S. arvensis* was relatively more tolerant to the extract of SH than *C. album*, while G_{max} of *S. arvensis* was 4% and 1% under 100 and 200 g L^{-1} SH extract and SH + $NOEC_{50}$ conditions, respectively, and the G_{max} of the other two species was stopped. In the presence of Fe_3O_4 NPs, the concentration of SH extract for the complete inhibition of germination of *C. album* increased from 100 g L^{-1} to 200 g L^{-1}.

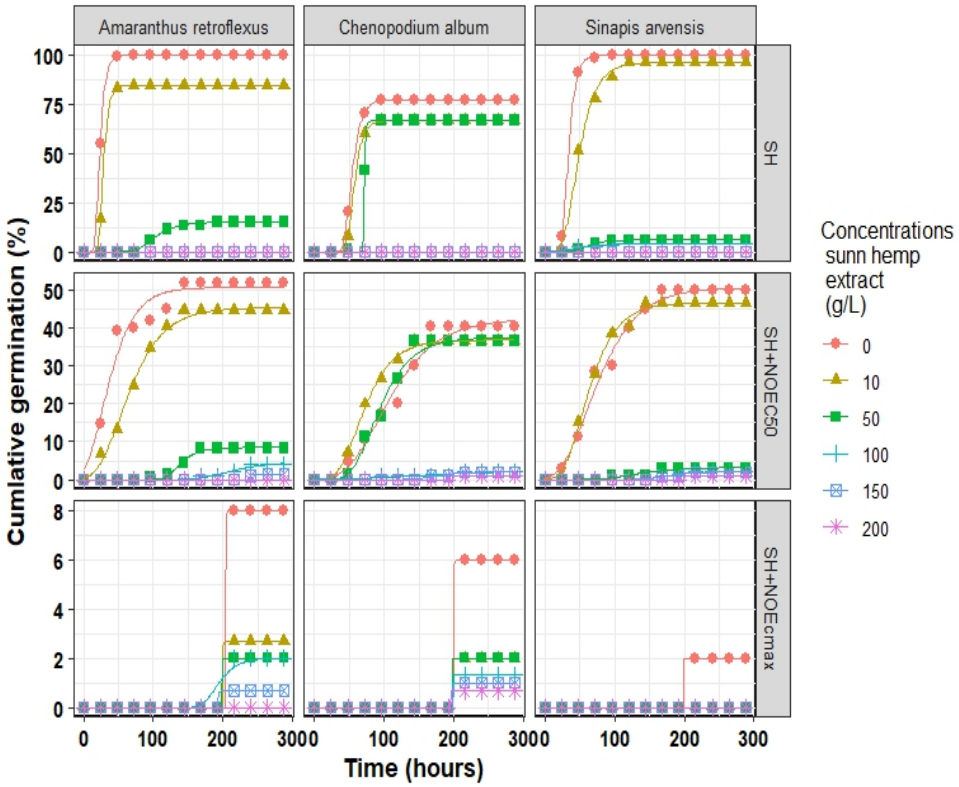

Figure 3. Cumulative germination of three weeds species influenced by different concentrations of sunn hemp extract (SH) and two points of Fe_3O_4/sunn hemp NPs ($NOEC_{50}$ and $NOEC_{max}$) fitted Gompertz model. The points correspond to the observed values, whereas the lines represent the predicted values. $NOEC_{50}$, half maximal effective concentration of Fe_3O_4/sunn hemp NPs; $NOEC_{max}$, maximal effective concentration of Fe_3O_4/sunn hemp NPs.

3.4. Optimizing Sunn Hemp Extract Effect

Figure 4 and Table 2 illustrate the fitted logistic model for optimizing the effect of SH extract on the G_{max} of all three weed species. Our findings indicated that the logistic model successfully fitted the G_{max} count and $1/D_{50}$ for all three weed species. The R^2 values ranged from 0.940 to 0.999 and RMSE values varied from 0.001 to 4.32 when different concentrations of SH extract were used, depending on the estimated parameter. For example, the maximum EEC_{50} (half maximal effective concentration) of SH extract for G_{max} was estimated at 23.9 g L^{-1} for *S. arvensis* but 52.3 g L^{-1} for *C. album.* The presence of Fe_3O_4 NPs resulted in an increase in EEC_{50} of *A. retroflexus* from 21.9 to 25.3 g L^{-1}, from 52.3 to 64.5 g L^{-1} in *C. album*, and from 23.9 to 21.7 g L^{-1} in *S. arvensis*. On the contrary, EEC_{50} for $1/D_{50}$ in *A. retroflexus* and *S. arvensis* decreased whereas in *C. album* increased in the presence of Fe_3O_4 NPs at the optimized point (Table 2).

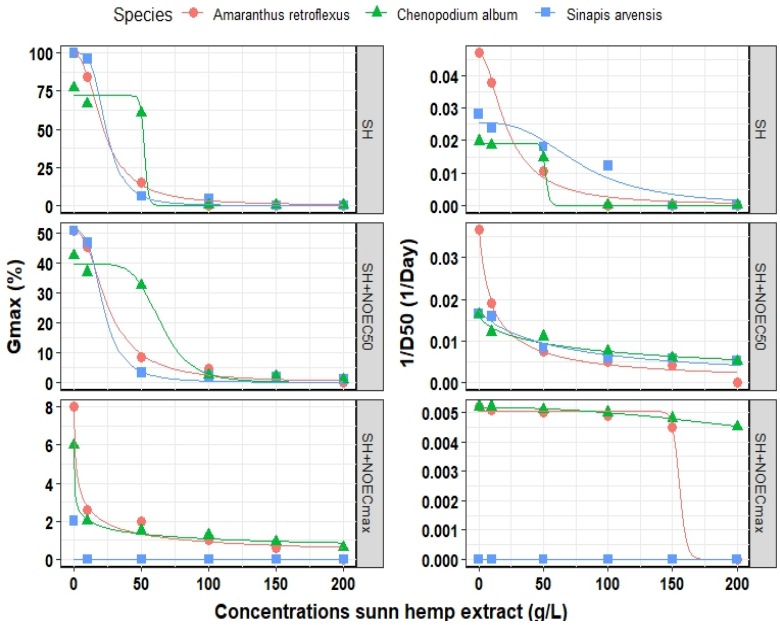

Figure 4. Final germination (G_{max}) and germination rate ($1/D_{50}$) of three weeds species influenced by different concentrations of sunn hemp extract and three points of Fe_3O_4/sunn hemp NPs (SH, SH + $NOEC_{50}$ and SH + $NOEC_{max}$) when fitted by logistic model. The points correspond to the observed values, whereas the lines represent the predicted values. SH, Sunn hemp extract; $NOEC_{50}$, half maximal effective concentration of Fe_3O_4/sunn hemp NPs; $NOEC_{max}$, maximal effective concentration of Fe_3O_4/sunn hemp NPs.

Table 2. Estimated parameters of final germination percentage (G_{max}) and germination rate ($1/D_{50}$) of three weed species influenced by different concentrations of sunn hemp extract and Fe_3O_4/sunn hemp NPs.

Species	Estimate Parameter	G_{max}			$1/D_{50}$		
		SH	SH+ $NOEC_{50}$	SH+ $NOEC_{max}$	SH	SH+ $NOEC_{50}$	SH+ $NOEC_{max}$
Amaranthus retroflexus	Y_{max}	99.6 ± 2.3	51.0 ± 1.5	8.0 ± 0.5	0.047 ± 0.002	0.037 ± 0.002	0.005 ± 0.0002
	EEC_{50}	21.9 ± 1.5	25.3 ± 2.4	3.6 ± 2.7	22.7 ± 3.2	11.0 ± 2.2	155.6 ± 25.4
	Slope	−2.3 ± 0.17	−2.2 ± 0.22	−0.61 ± 0.20	−1.88 ± 0.26	−0.92 ± 0.12	−57.6 ± 4.63
	R^2	0.999	0.998	0.979	0.994	0.992	0.997
	RMSE	2.24	1.49	0.54	0.002	0.002	0.0001
Sinapis arvensis	Y_{max}	99.9 ± 1.9	50.9 ± 1.5	-	0.026 ± 0.003	0.017 ± 0.001	-
	EEC_{50}	23.9 ± 2.5	21.7 ± 2.3	-	78.3 ± 15.8	62.8 ± 17.8	-
	Slope	−3.6 ± 0.47	−3.0 ± 0.40	-	−2.8 ± 1.2	−0.96 ± 0.24	-
	R^2	0.999	0.998	-	0.940	0.962	-
	RMSE	1.95	1.48	-	0.004	0.001	-
Chenopodium album	Y_{max}	72.0 ± 2.50	39.7 ± 1.8	6.0 ± 0.2	0.019 ± 0.007	0.016 ± 0.001	0.005 ± 0.0001
	EEC_{50}	52.3 ± 3.61	64.5 ± 5.3	1.9 ± 1.4	51.3 ± 6.52	83.4 ± 3.2	523.4 ± 57.4
	Slope	−36.0 ± 4.60	−5.8 ± 1.6	−0.38 ± 0.08	−35.5 ± 4.90	−0.73 ± 0.09	−1.97 ± 0.21
	R^2	0.992	0.990	0.992	0.998	0.977	0.996
	RMSE	4.32	2.59	0.22	0.004	0.001	0.0002

Y_{max}, G_{max}, or $1/D_{50}$ in distilled water; G_{max}, Final germination percentage, D_{50}, Time to reach 50% germination; SH, Sunn hemp extract; $NOEC_{50}$, Half maximal effective concentration of Fe_3O_4/sunn hemp NPs; $NOEC_{max}$, Maximal effective concentration of Fe_3O_4/sunn hemp NPs; EEC_{50}, Half maximal effective concentration of treatments; RMSE, Root Square Error; R^2, Coefficient of determination.

3.5. Extract Components

Table 3 displays the results of the sunn hemp GC-MS analysis utilized in this experiment. The analysis identified 37 dominant components in the extract, with Nonadecane (105.8 mg/g), Heneicosane (58.1 mg/g), Pentadecanone, 6, 10, 14-trimethyl (33.3 mg/g), Heptadecane (31.8 mg/g), Triallylsilane (33.7 mg/g), Phytol (39.5 mg/g), and Crotonic acid, Menthyl ester (35.4 mg/g) being the most prevalent compounds. Among these components, nonadecane was the dominant compound, with concentration (0.06–21.16 g L^{-1}) across concentrations of sunn hemp, ranging from 10 to 200 g L^{-1}. Interestingly, the concentrations of the other components of the extract remained relatively constant.

Table 3. GC-MS results for sunn hemp at the minimum and maximum tested concentrations [45].

Row	Components	Time	Plant Content (mg/g)	Extract Content	
				Min (mg/L)	Max (mg/L)
1	Naphthalene	14.9	11.9	0.06	2.38
2	Apha-Cubebene	18.3	7	0.04	1.40
3	Caryophyllene	19.2	7.5	0.04	1.50
4	H-Cyclopropa[a]naphthalene	19.5	10.7	0.05	2.14
5	5,9-Undecadien-2-one, 6,10-dimet	19.9	8.3	0.04	1.66
6	Hexadecane	20.1	5.6	0.03	1.12
7	1,2,4-Methenoazulene, decahydro	20.6	6.9	0.03	1.38
8	Buten-2-one, 4-2,6,6-trimethy	20.7	13.8	0.07	2.76
9	Caryophyllene oxide	22.7	11.7	0.06	2.34
10	Cyclohexane, 1,1,3,5-tetramethyl	22.8	5.7	0.03	1.14
11	Heptadecane	24.7	31.8	0.16	6.36
12	Octadecane	26.5	5.1	0.03	1.02
13	Pentadecanone, 6,10,14-trimethyl	27.3	33.3	0.17	6.66
14	Z-5-Nonadecene	27.8	13.4	0.07	2.68
15	Nonadecane	28.3	105.8	0.53	21.16
16	5,9, 13-Pentadecatrien-2-one, 6,1	28.6	11.5	0.06	2.30
17	Triallylsilane	29.1	33.7	0.17	6.74
18	N-Hexadecanoic acid	29.3	8.5	0.04	1.70
19	Eicosane	29.8	19.2	0.10	3.84
20	Heneicosane	31.4	58.1	0.29	11.62
21	Phytol	31.6	39.5	0.20	7.90
22	Dodecane, 1-cyclopentyl-4-3-cyc	32.9	28.2	0.14	5.64
23	Cyclohexane, 1-ethyl-2-propyl	35.1	10.8	0.05	2.16
24	Cyclohexane, 1,1′-methylenebis	35.6	6	0.03	1.20
25	Triallylsilane	36.4	20.5	0.10	4.10
26	Tetracosane	41.5	12.1	0.06	2.42
27	Cyclohexane, 1,1′-propylidenebis	43.3	17.5	0.09	3.50
28	Eicosane, 3-cyclohexyl	43.4	14.5	0.07	2.50
29	Cyclooctane, 1-methyl-3-propyl	43.9	7.7	0.04	1.54
30	Cyclohexane, (1-decylundecyl)	44.2	16.3	0.08	3.26
31	Phosphorous acid, tris (decyl) ester	44.3	11.6	0.06	2.32
32	Cyclohexane, 2,4-diethyl-1-methyl	44.4	7.1	0.04	1.42
33	Decane, 5, 6-bis 2,2-dimethylprop	44.9	6.3	0.03	1.26
34	Benzene, 1-fluoro-2-methoxy	45.6	24.5	0.12	4.90
35	Crotonic acid, menthyl ester	45.7	35.4	0.18	7.08
36	1,2-Dodecanediol	46.2	6.6	0.03	1.32
37	Octen-2-one, 3,6-dimethyl	46.3	28.8	0.14	5.76

4. Discussion

Biosynthesis of NPs using plant extracts with allelopathic properties is cost-effective and environmentally friendly, and can be implemented as an alternative to synthetic

herbicides for weed management [46,47]. This study evaluates the effectiveness of using green synthesis of Fe_3O_4 NPs with allelopathic sunn hemp (SH) extract in inhibiting the germination of three common weeds.

Our results demonstrated that SH aqueous extract, Fe_3O_4 NPs, and Fe_3O_4/sunn hemp NPs considerably inhibited the germination of *A. retroflexus*, *S. arvensis*, and *C. album*. The extent of inhibition, however, varied among species, reflecting differences in sensitivity. This variation in germination potential is among species' inherent biological differences and ecological adaptations that influence their competitive abilities in agricultural settings [48–50]. As our results exhibited, *A. retroflexus* had the highest sensitivity to SH extract among other species, whereas *C. album* displayed relative tolerance. This variability in response may stem from differences in seed coat permeability and water absorption mechanisms, as thicker seed coats in *C. album* likely limited water and allelochemical uptake [51], and *C. album* had 77% germinating rate in control conditions.

Sunn hemp extract, notably lowered G_{max} while raising the $1/D_{50}$ values for all three weed species, suggesting a delay in the time needed to achieve 50% germination. Sunn hemp extracts inhibited germination because allelochemicals can hinder endosperm weakening and embryo growth (processes required for endosperm rupture and root protrusion) [52,53]. Gas chromatography–mass spectrometry (GC-MS) analysis of SH extract identified phytol, terpenes, and other compounds; however, isolating individual compounds is necessary to elucidate their specific modes of action. Prior research has indicated that the SH aqueous extract contains a variety of phytochemicals, including alkaloids, and flavonoids [18,54]. Prior studies reported that alkaloids impact seeds by hindering water uptake, disrupting germination enzymes, and affecting hormonal balance [55]. The effect of phenolic compounds varies by their concentration and receptor sensitivity. Additionally, flavonoids inhibit germination by disrupting cell membrane permeability and causing leakage [56,57]. Our results are aligned with Skinner et al. [25], and Abdelmalik et al. [58], who found that dried ground sunn hemp residues and leaf extracts inhibited germination and seedling growth of various weeds and cover crops and also that there is a correlation between extract concentration and reduced germination.

The comprehensive characterization of Fe_3O_4 NPs synthesized using SH extract underscores the adaptability of these materials. Analytical techniques, including XRD, SEM, FTIR, TGA, BET, and VSM, demonstrated the structural integrity, presence of functional groups, microstructural features, thermal stability, surface characteristics, and magnetic properties of the NPs. The findings affirmed the viability of employing SH extracts for functionalization, highlighting the practical potential of NP synthesis with SH [59]. The results of this study indicated that in optimizing the Fe_3O_4 NPs effect in the control group, G_{max} ranged from 100 to 77% for *A. retroflexus*, *S. arvensis*, and *C. album*. Germination significantly decreased by 80–68% at the highest Fe_3O_4 NPs concentration (3000 mg L^{-1}), while concentrations up to 200 mg L^{-1} did not inhibit germination in these three weed species (Figure 2). These findings suggest that low concentrations of Fe_3O_4 NPs do not inhibit seed germination and therefore may not significantly threaten weed establishment. However, a high concentration of Fe_3O_4 NPs (3000 mg L^{-1}) significantly reduced germination, possibly due to insufficient interaction of the functional groups of the NPs at this level. The functional groups of Fe_3O_4 NPs effective in stabilizing reactive oxygen species (ROS) during seed germination mainly include oxygen-containing groups (COOH-, OH-, C=O, and -O) that interact with ROS and regulate oxidative stress [60]. Fourier-transform infrared spectroscopy (FTIR) analysis of Fe_3O_4 NPs revealed C-O and O-H bonds (Figure 1e), yet there was probably insufficient interaction to neutralize radicals and control ROS at high Fe_3O_4 NPs concentrations, led to a severe reduction and inhibiting seeds germination. These findings align with previous research [61], which indicated that *Parthenium*-mediated

green synthesis of Fe_3O_4 NPs greatly reduced corn seed germination at 400 ppm, while lower concentrations acted as micronutrients. Additionally, based on the $NOEC_{50}$ results, *A. retroflexus* seeds demonstrated the highest tolerance to Fe_3O_4 NPs. Increased Fe_3O_4 NPs concentration reduces seed germination in *A. retroflexus*, *S. arvensis*, and *C. album*. Despite the high concentrations utilized in this study, it is noteworthy that the evaluated weed species did not show statistically significant differences in $NOEC_{max}$ values. This underscores the toxic effects of elevated concentrations of Fe_3O_4 NPs, necessitating further research into the mechanisms of action of seeds against Fe_3O_4 NPs. Another report indicated that high concentrations of Fe_3O_4 ($\geq$100 mg L^{-1}) exacerbated oxidative stress markers (malondialdehyde, H_2O_2) in rice seedlings [62]. Our findings are also aligned with Kornarzyński et al. [63], who investigated the effects of Fe_3O_4 NPs on seed germination and element concentration in *Helianthus annuus* L., reporting Fe_3O_4 NPs' toxic effects on the reduction of germination parameters.

Green-synthesized Fe_3O_4 NPs with SH extract (SH + $NOEC_{50}$) reduced or completely stopped the germination of *S. arvensis*, *C. album*, and *A. retroflexus*. In addition to the varying sensitivities of weed seeds to SH extract, Fe_3O_4 NPs, and Fe_3O_4/sunn hemp NPs, increasing the concentration of Fe_3O_4/sunn hemp NPs reduced or eliminated germination. This reduction in germination is likely due to the decreased NP surface area at higher extract concentrations. As shown by the BET results (Table 1), surface area decreases for Fe_3O_4/sunn hemp (15% and 20%) NPs with increasing extract concentration. The reduced BET surface area of green synthesized Fe_3O_4 NPs with SH extract may hinder seed germination by limiting water and NPs uptake, interaction with seeds, and possibly nutrient delivery [63,64]. However, increasing SH concentration in the Fe_3O_4 green synthesis enhanced the functional groups (C-O and O-H) (Figure 1e). In this study, the observed reduction in NPs surface area at 15% and 20% concentrations (150 and 200 g L^{-1}) may limit the interaction of these functional groups, reducing their ability to alleviate oxidative stress during germination [60,65]. While Fe_3O_4 NPs can have both positive and negative effects on germination [66–68], the unique properties of Fe_3O_4 NPs, including their small size, high surface area, modifiable surface, functional groups, and magnetic properties, likely influence their mechanism of action [69]. For instance, one study found that root water uptake decreased to 57% of the control at 50 mg L^{-1} and further decreased to 26% at 100 mg L^{-1} [63].

5. Conclusions

The use of natural products, such as plant extracts, for weed control has gained popularity due to their short environmental half-lives, low toxicity, and eco-friendliness. This study examined the effectiveness of sunn hemp leaf extract, Fe_3O_4 NPs, and their green synthesis on the seed germination of three globally common weeds. Weed species exhibited variable responses to sunn hemp extracts, Fe_3O_4 NPs, and Fe_3O_4/sunn hemp NPs, underscoring the importance of tailoring weed management strategies to specific species. The combination of Fe_3O_4 NPs and sunn hemp extract enhanced their inhibitory effects on weed germination, suggesting a synergistic interaction between nanoparticles and allelochemicals. Understanding the mechanisms underlying these differences, such as seed coat permeability, functional groups of NPs, and water absorption, may improve the efficacy of natural herbicides. The results indicated that the concentration of NPs and sunn hemp extract plays a critical role in their effectiveness. While low concentrations had minimal impact, higher concentrations significantly inhibited germination, emphasizing the need for precise dosing in practical applications.

Author Contributions: Conceptualization, M.H. and F.A.; methodology, F.A. and M.T.A.; software, F.A., S.F. and G.P.; validation, M.H.; formal analysis, G.P. and F.A.; investigation, F.A.; resources, M.H., F.A. and S.F.; data curation, F.A. and G.P.; writing—original draft preparation, F.A. and M.H.; writing—review and editing, M.H., F.A., A.E. and G.P.; visualization, M.H.; supervision, M.H.; project administration, F.A.; funding acquisition, M.H. and A.E. All authors have read and agreed to the published version of the manuscript.

Funding: This research received no external funding.

Data Availability Statement: The data that supports the findings of this study are available from the corresponding author upon reasonable request.

Acknowledgments: The authors gratefully acknowledge the support from the Faculty of Agricultural Sciences and Natural Resources at the University of Mohaghegh Ardabili, Iran, and the Stockbridge School of Agriculture at the University of Massachusetts Amherst, USA.

Conflicts of Interest: The authors declare no conflicts of interest. The funders had no role in the design of the study; in the collection, analyses, or interpretation of data; in the writing of the manuscript; or in the decision to publish the results.

Abbreviations

The following abbreviations are used in this manuscript:

BET	Brunner–Emmet–Teller
EEC_{50}	Half-maximal effective concentration
FTIR	Fourier-transform infrared spectroscopy
GC-MS	Gas chromatography–mass spectrometry
G_{max}	Final germination percentage or Maximum germination
$NOEC_{50}$	Half maximal effective concentration of Fe_3O_4 NPs and Fe_3O_4/sunn hemp NPs
$NOEC_{max}$	The maximal effective concentration of Fe_3O_4 NPs and Fe_3O_4/sunn hemp NPs
NPs	Nanoparticles
SEM	Scanning electron microscopy
SH	Sunn hemp extract
TGA	Thermogravimetric analysis
VSM	Vibrating sample magnetometer
XRD	Scanning X-ray diffraction

Appendix A

Table A1. Estimated parameters of cumulative germination changes on *A. retroflexus* influenced by different concentrations of sunn hemp extract and Fe_3O_4/sunn hemp NPs.

Sunn Hemp Extract Concentrations (g L^{-1})	Sunn Hemp Aqueous Extract					Fe_3O_4/Sunn Hemp NPs									
	SH					SH + $NOEC_{50}$					SH + $NOEC_{max}$				
	Estimate Parameter			R^2	RMSE	Estimate Parameter			R^2	RMSE	Estimate Parameter			R^2	RMSE
	G_{max} (%)	D_{50} (h)	Slope			G_{max} (%)	D_{50} (h)	Slope			G_{max} (%)	D_{50} (h)	Slope		
0	99.9 ± 0.05	21.3 ± 0.01	5.3 ± 0.01	0.999	0.002	50.8 ± 1.3	27.3 ± 3.6	25.8 ± 7.7	0.961	3.54	8.0 ± 0.00	192.6 ± 0.39	0.30 ± 0.02	0.999	0.001
10	84.6 ± 0.01	26.5 ± 0.02	5.2 ± 0.01	0.999	0.004	45.5 ± 0.5	52.7 ± 1.7	33.5 ± 2.3	0.995	1.25	2.6 ± 0.00	196.1 ± 0.30	0.36 ± 0.02	0.999	0.001
50	15.1 ± 0.24	95.5 ± 1.74	21.0 ± 2.0	0.995	0.530	8.5 ± 0.2	133.6 ± 2.1	16.7 ± 2.5	0.991	0.41	2.0 ± 0.00	200.1 ± 0.30	0.30 ± 0.01	0.999	0.002
100	-	-	-	-	-	4.7 ± 3.2	200.7 ± 8.1	38.0 ± 10.6	0.859	0.34	1.0 ± 0.00	204.8 ± 0.36	0.30 ± 0.01	0.995	0.067
150	-	-	-	-	-	1.4 ± 3.2	239.4 ± 2.7	38.2 ± 1.3	0.999	0.01	0.6 ± 0.00	222.1 ± 0.34	0.26 ± 0.01	0.999	0.002
200	-	-	-	-	-	-	-	-	-	-	-	-	-	-	-

G_{max}, Final germination; D_{50}, Time to reach 50% germination; SH, Sunn hemp extract; $NOEC_{50}$, Half maximal effective concentration of Fe_3O_4/sunn hemp NPs; $NOEC_{max}$, Maximal effective concentration of Fe_3O_4/sunn hemp NPs; RMSE, Root Mean Square Error; R^2, Coefficient of determination.

Table A2. Estimated parameters of cumulative germination changes on *S. arvensis* influenced by different concentrations of sunn hemp extract and Fe_3O_4/sunn hemp NPs.

Sunn Hemp Extract Concentrations (g L^{-1})	Sunn Hemp Aqueous Extract					Fe_3O_4/Sunn Hemp NPs									
	SH					SH + $NOEC_{50}$					SH + NOECmax				
	Estimate Parameter			R^2	RMSE	Estimate Parameter			R^2	RMSE	Estimate Parameter			R^2	RMSE
	G_{max} (%)	D_{50} (h)	Slope			G_{max} (%)	D_{50} (h)	Slope			G_{max} (%)	D_{50} (h)	Slope		
0	99.8 ± 0.01	30.6 ± 0.11	7.2 ± 0.01	0.999	0.30	50.8 ± 1.10	60.9 ± 2.9	38.7 ± 4.1	0.989	2.17	2.0 ± 0.00	198.2 ± 0.29	0.05 ± 0.02	0.999	0.001
10	96.2 ± 0.87	42.1 ± 1.17	16.8 ± 1.4	0.996	2.49	46.8 ± 0.47	63.0 ± 1.4	27.0 ± 1.8	0.996	1.16	-	-	-	-	-
50	6.0 ± 0.06	55.3 ± 1.08	15.9 ± 1.3	0.996	0.16	3.2 ± 0.29	121.2 ± 9.0	39.8 ± 9.2	0.934	0.39	-	-	-	-	-
100	3.9 ± 0.12	69.9 ± 4.05	21.5 ± 5.0	0.958	0.33	2.0 ± 0.13	169.0 ± 4.8	26.3 ± 7.2	0.971	0.17	-	-	-	-	-
150	-	-	-	-	-	1.9 ± 0.03	172.0 ± 1.3	26.3 ± 7.2	0.921	0.14	-	-	-	-	-
200	-	-	-	-	-	1.0 ± 0.03	199.0 ± 0.8	0.26 ± 0.2	0.999	0.00	-	-	-	-	-

G_{max}, Final germination; D_{50}, Time to reach 50% germination; SH, Sunn hemp extract; $NOEC_{50}$, Half maximal effective concentration of Fe_3O_4/sunn hemp NPs; $NOEC_{max}$, Maximal effective concentration of Fe_3O_4/sunn hemp NPs; RMSE, Root Mean Square Error; R^2, Coefficient of determination.

Table A3. Estimated parameter of cumulative germination change on *C. album* influenced by different concentrations of sunn hemp extract and Fe_3O_4/sunn hemp NPs.

Sunn Hemp Extract Concentrations (g L^{-1})	Sunn Hemp Aqueous Extract					Fe_3O_4/Sunn Hemp NPs									
	SH					SH + $NOEC_{50}$					SH + $NOEC_{max}$				
	Estimate Parameter			R^2	RMSE	Estimate Parameter			R^2	RMSE	Estimate Parameter			R^2	RMSE
	G_{max} (%)	D_{50} (h)	Slope			G_{max} (%)	D_{50} (h)	Slope			G_{max} (%)	D_{50} (h)	Slope		
0	77.3 ± 0.05	50.7 ± 0.04	8.8 ± 0.07	0.999	0.14	42.6 ± 1.72	61.3 ± 1.32	45.9 ± 7.12	0.982	2.49	6.0 ± 0.001	192.6 ± 0.38	0.35 ± 0.02	0.999	0.001
10	66.7 ± 0.03	54.0 ± 0.05	7.9 ± 0.04	0.999	0.10	36.9 ± 0.36	82.9 ± 2.92	27.5 ± 1.73	0.997	0.87	2.0 ± 0.001	192.5 ± 0.38	0.05 ± 0.02	0.999	0.001
50	60.6 ± 0.15	68.7 ± 1.24	1.6 ± 0.085	0.999	0.42	32.5 ± 0.89	90.9 ± 4.68	30.2 ± 3.98	0.989	1.85	1.5 ± 0.001	196.0 ± 0.35	0.06 ± 0.01	0.999	0.001
100	-	-	-	-	-	2.5 ± 0.70	134.9 ± 32.7	87.8 ± 42.2	0.893	0.29	1.3 ± 0.002	200.1 ± 0.30	0.30 ± 0.01	0.999	0.001
150	-	-	-	-	-	2.0 ± 0.13	169.0 ± 4.8	26.3 ± 7.2	0.971	0.17	0.9 ± 0.002	208.3 ± 0.40	0.26 ± 0.01	0.999	0.001
200	-	-	-	-	-	1.0 ± 0.13	199.8 ± 2.4	0.26 ± 0.2	0.999	0.001	0.6 ± 0.001	221.2 ± 0.35	0.19 ± 0.01	0.999	0.001

G_{max}, Final germination; D_{50}, Time to reach 50% germination; SH, Sunn hemp extract; $NOEC_{50}$, Half maximal effective concentration of Fe_3O_4/sunn hemp NPs; $NOEC_{max}$, Maximal effective concentration of Fe_3O_4/sunn hemp NPs; RMSE, Root Mean Square Error; R^2, Coefficient of determination.

References

1. Kostina-Bednarz, M.; Plonka, J.; Barchanska, H. Allelopathy as a source of bioherbicides: Challenges and prospects for sustainable agriculture. *Rev. Environ. Sci. Biotechnol.* **2023**, *22*, 471–504. [CrossRef]
2. Yadav, T.; Chopra, N.K.; Chopra, N.K.; Kumar, R.; Soni, P.G. Assessment of critical period of crop-weed competition in forage cowpea (*Vigna unguiculata*) and its effect on seed yield and quality. *Indian J. Agron.* **2018**, *63*, 124–127.
3. Hunter, J.E.; Gannon, T.W.; Richardson, R.J.; Yelverton, F.H.; Leon, R.G. Integration of remote-weed mapping and an autonomous spraying unmanned aerial vehicle for site-specific weed management. *Pest. Manag. Sci.* **2020**, *76*, 1386–1392. [CrossRef]
4. Esposito, M.; Crimaldi, M.; Cirillo, V.; Sarghini, F.; Maggio, A. Drone and sensor technology for sustainable weed management: A review. *Chem. Biol. Technol. Agric.* **2021**, *8*, 18. [CrossRef]
5. Gawel, A.; Seiwert, B.; Sühnholz, S.; Schmitt-Jansen, M.; Mackenzie, K. In-situ treatment of herbicide-contaminated groundwater–Feasibility study for the cases atrazine and bromacil using two novel nanoremediation-type materials. *J. Hazard. Mater.* **2020**, *393*, 1–10. [CrossRef]
6. Li, Z.F.; Dong, J.X.; Vasylieva, N.; Cui, Y.L.; Wan, D.B.; Hua, X.D.; Huo, J.Q.; Yang, D.C.; Gee, S.J.; Hammock, B.D. Highly specific nanobody against herbicide 2,4-dichlorophenoxyacetic acid for monitoring of its contamination in environmental water. *Sci. Total Environ.* **2021**, *753*, 141950. [CrossRef] [PubMed]
7. Ghahremani, S.; Ebadi, A.; Tobeh, A.; Hashemi, M.; Sedghi, M.; Gholipoouri, A.; Barker, V. Short-term impact of monoculture and mixed cover crops on soil properties, weed suppression, and lettuce yield. *Commun. Soil. Sci. Plant Anal.* **2021**, *52*, 406–415. [CrossRef]
8. Yadav, A.S.; Srivastava, D.S. Application of nano-technology in weed management: A Review. *Res. Rev. J. Crop Sci. Technol.* **2015**, *4*, 21–23.
9. Choudhary, S.K.; Kumar, A.; Kumar, R. Novel nanotechnological tools for weed management—A review. *Chem. Rev. Lett.* **2020**, *9*, 886–894.
10. Mondal, P.; Anweshan, A.; Purkait, M.K. Green synthesis and environmental application of iron-based nanomaterials and nanocomposite: A review. *Chemosphere* **2020**, *259*, 1–111. [CrossRef]
11. Markova, Z.; Novak, P.; Kaslik, J.; Plachtova, P.; Brazdova, M.; Jancula, D.; Siskova, K.; Machala, L.; Marsalek, B.; Zboril, R.; et al. Iron (II, III)-Polyphenol complex nanoparticles derived from green tea with remarkable ecotoxicological impact. *ACS Sustain. Chem. Eng.* **2014**, *2*, 1674–1680. [CrossRef]
12. Luo, F.; Chen, Z.; Megharaj, M.; Naidu, R. Biomolecules in grape leaf extract involved in one-step synthesis of iron-based nanoparticles. *RSC Adv.* **2014**, *96*, 53467–53474. [CrossRef]
13. Besançon, T.E.; Wasacz, M.H.; Heckman, J.R. Weed suppression, nitrogen availability, and cabbage production following Sunn hemp or Sorghum-Sudan grass. *HortTechnology* **2021**, *31*, 439–447. [CrossRef]
14. Cho, A.H.; Chase, C.A.; Treadwell, D.D.; Koenig, R.L.; Morris, J.B.; Morales-Payan, J.P. Apical dominance and planting density effects on weed suppression by Sunn Hemp (*Crotalaria juncea* L.). *HortScience* **2015**, *50*, 263–267. [CrossRef]
15. Parenti, A.; Cappelli, G.; Zegada-Lizarazu, W.; Sastre, C.M.; Christou, M.; Monti, A.; Ginaldi, F. SunnGro: A new crop model for the simulation of Sunn hemp (*Crotalaria juncea* L.) grown under alternative management practices. *Biomass Bioenergy* **2021**, *146*, 1–16. [CrossRef]
16. Meagher, R.L.; Rodney, J.R.; Nagoshi, N.; Brown, J.T. Flowering of the cover crop Sunn hemp, *Crotalaria juncea* L. *HortScience* **2017**, *52*, 986–990. [CrossRef]
17. Bundit, A.; Ostlie, M.; Prom-U-Thai, C. Sunn hemp (*Crotalaria juncea*) weed suppression and allelopathy at different timings. *Biocontrol Sci. Technol.* **2021**, *31*, 694–704. [CrossRef]
18. Javaid, M.M.; Bhan, M.; Johnson, J.V.; Rathinasabapathi, B.; Chase, C.A. Biological and chemical characterizations of allelopathic potential of diverse accessions of the cover crop Sunn hemp. *J. Am. Soc. Hortic. Sci.* **2015**, *140*, 532–541. [CrossRef]
19. Morris, J.B.; Chase, C.; Treadwell, D.; Koenig, R.; Cho, A.; Morales-Payan, J.P.; Murphy, T.; Antonious, G.F. Effect of Sunn hemp (*Crotalaria juncea* L.) cutting date and planting density on weed suppression in Georgia, USA. *J. Environ. Sci. Health [B]* **2015**, *50*, 614–621. [CrossRef]
20. Colegate, S.M.; Gardner, D.R.; Joy, R.J.; Betz, J.M.; Panter, K.E. Dehydropyrrolizidine alkaloids, including monoesters with an unusual esterifying acid, from cultivated *Crotalaria juncea* (Sunn hemp cv. 'Tropic Sun'). *J. Agric. Food Chem.* **2012**, *60*, 3541–3550. [CrossRef]
21. Adams, R.; Gianturco, M. The alkaloids of *Crotalaria juncea*. *J. Am. Chem. Soc.* **1956**, *78*, 1919–1921. [CrossRef]
22. Li, A.; Zheng, R.; Tian, L.; Wei, Y.; Wu, J.; Hou, X. Allelopathic effects of switchgrass on redroot pigweed and crabgrass growth. *J. Plant Ecol.* **2021**, *222*, 1–12. [CrossRef]

23. Mousavi, S.A.; Feizi, H.; Ahmadian, A.; Izadi Darbandi, E. Extracts obtained from organs of saffron (*Crocus sativus*) alter growth and seed germination of common lamb's quarters (*Chenopodium album*) and barnyard grass *(Echinochloa crus-galli*). *Plant Biosyst.-An. Int. J. Deal. All Asp. Plant Biol.* **2023**, *157*, 1–8. [CrossRef]
24. Boukhili, M.; Szilágyi, A.; Cheradil, A. Allelopathic effect of five invasive plants on seed germination and growth of wild mustard. *Rev. Agric. Rural. Dev.* **2022**, *11*, 1–5. [CrossRef]
25. Skinner, E.M.; Díaz-Pérez, J.C.; Phatak, S.C.; Schomberg, H.H.; Vencill, W. Allelopathic effects of Sunn hemp (*Crotalaria juncea* L.) on germination of vegetables and weeds. *HortScience* **2012**, *47*, 138–142. [CrossRef]
26. Rotar, P.P.; Joy, R.J. *'Tropic Sun' Sunn Hemp (Crotalaria juncea L.)*; Research Extension Series; University of Hawaii: Honolulu, HI, USA, 1983.
27. Iftikhar Hussain, M.; El-Sheikh, M.A.; Reigosa, M.J. Allelopathic potential of aqueous extract from *Acacia melanoxylon* R. Br. on *Lactuca sativa*. *Plants* **2020**, *9*, 1228. [CrossRef] [PubMed]
28. Trusheva, B.; Trunkova, D.; Bankova, V. Different extraction methods of biologically active components from propolis: A preliminary study. *Chem. Cent. J.* **2007**, *1*, 1–4. [CrossRef]
29. Babaei-Ghaghelestany, A.; Alebrahim, M.T.; MacGregor, D.R.; Khatami, S.A.; Hasani Nasab Farzaneh, R. Evaluation of ultrasound technology to break seed dormancy of common lamb's quarters (*Chenopodium album*). *Food Sci. Nutr.* **2020**, *8*, 2662–2669. [CrossRef]
30. Ahmadnia, F.; Alebrahim, M.T.; Nabati Souha, L.; MacGregor, D.R. Evaluation of techniques to break seed dormancy in Redroot pigweed (*Amaranthus retroflexus*). *Food Sci. Nutr.* **2024**, *12*, 2334–2345. [CrossRef]
31. Şin, B.; Kadıoğlu, I. A Study on germination biology of Wild Mustard (*Sinapis arvensis* L.). *Turk. J. Agric.-Food Sci. Technol.* **2021**, *9*, 728–732. [CrossRef]
32. Massart, R. Preparation of aqueous magnetic liquids in alkaline and acidic media. *IEEE Trans. Magn.* **1981**, *17*, 1247–1248. [CrossRef]
33. Perry, D. Methodology and application of vigour tests. In *Handbook of Vigour Test Methods International Seed Testing Association*; International Seed Testing Association: Wallisellen, Switzerland, 1981; pp. 3–7.
34. Scott, S.; Jones, R.; Williams, W. Review of data analysis methods for seed germination 1. *Crop Sci.* **1984**, *24*, 1192–1199. [CrossRef]
35. Burnett, S.E.; Pennisi, S.V.; Thomas, P.A.; Van Iersel, M.W. Controlled drought affects morphology and anatomy of *Salvia splendens*. *J. Am. Soc. Hortic. Sci.* **2005**, *130*, 775–781.
36. Antarnusa, G.; Jayanti, P.D.; Denny, Y.R.; Suherman, A. Utilization of co-precipitation method on synthesis of Fe_3O_4/PEG with different concentrations of PEG for biosensor applications. *Materialia* **2022**, *25*, 101525. [CrossRef]
37. Zhang, Q.; Li, S.; Zhang, W.; Peng, K. Influence of processed parameters on the magnetic properties of Fe/Fe_3O_4 composite cores. *J. Mater. Sci.: Mater. Electron.* **2021**, *32*, 1233–1241. [CrossRef]
38. Sahu, S.R.; Jagannatham, M.; Gautam, R.; Rikka, V.R.; Prakash, R.; Mallikarjunaiah, K.J.; Reddy, G.S. A facile synthesis of raspberry-shaped Fe_3O_4 nanoaggregate and its magnetic and lithium-ion storage properties. *Mater. Sci. Eng. B* **2022**, *282*, 115771. [CrossRef]
39. Bhuiyan, M.S.H.; Miah, M.Y.; Paul, S.C.; Aka, T.D.; Saha, O.; Rahaman, M.M.; Sharif, M.J.I.; Habiba, O.; Ashaduzzaman, M. Green synthesis of iron oxide nanoparticle using *Carica papaya* leaf extract: Application for photocatalytic degradation of remazol yellow RR dye and antibacterial activity. *Heliyon* **2020**, *6*, e04603. [CrossRef] [PubMed]
40. Elgorban, A.M.; Marraiki, N.; Akber Ansari, S.; Syed, A. Green synthesis of Cu/Fe_3O_4 nanocomposite using *Calendula* extract and evaluation of its catalytic activity for chemo selective oxidation of sulfides to sulfoxides with aqueous hydrogen peroxide. *J. Org. Chem.* **2021**, *954–955*, 122077. [CrossRef]
41. Tiama, T.M.; Ismail, A.M.; Elhaes, H.; Ibrahim, M.A. Structural and spectroscopic studies for chitosan/Fe_3O_4 nanocomposites as glycine biosensors. *Biointerface Res. Appl. Chem.* **2023**, *13*, 547. [CrossRef]
42. Sari, E.K.; Tumbelaka, R.M.; Ardiyanti, H.; Istiqomah, N.I.; Chotimah Suharyadi, E. Green synthesis of magnetically separable and reusable Fe_3O_4/Cdots nanocomposites photocatalyst utilizing *Moringa oleifera* extract and watermelon peel for rapid dye degradation. *Carbon. Resour. Convers.* **2023**, *6*, 274–286. [CrossRef]
43. Inbaraj, B.S.; Chen, B.Y.; Liao, C.W.; Chen, B.H. Green synthesis, characterization and evaluation of catalytic and antibacterial activities of chitosan, glycol chitosan and poly (γ-glutamic acid) capped gold nanoparticles. *Int. J. Biol. Macromol.* **2020**, *161*, 1484–1495. [CrossRef] [PubMed]
44. Chen, J.; Wei, D.; Liu, L.; Nai, J.; Liu, Y.; Xiong, Y.; Peng, J.; Mahmud, S.; Liu, H. Green synthesis of *Konjac glucomannan* templated palladium nanoparticles for catalytic reduction of azo compounds and hexavalent chromium. *Mater. Chem. Phys.* **2021**, *267*, 124651. [CrossRef]

45. Ahmadnia, F.; Ebadi, A.; Hashemi, M.; Ghavidel, A.; Alebrahim, M.T. Investigating the effect of aqueous extracts of Sunn hemp (*Crotalaria juncea*) and Oats (*Avena sativa* L.) on the germination of wild mustard weed (*Sinapis arvensis*). *Iran. J. Seed Sci. Res.* **2023**, *10*, 1–19.
46. Ojo, S.K.S.; Otugboyega, J.O.; Ayo, I.O.; Ojo, A.M.; Oluwole, B.R. Mitigating Action of Nanobioherbicides from Natural Products on Agricultural Produce. In *Handbook of Agricultural Biotechnology*; John Wiley & Sons, Inc.: Hoboken, NJ, USA, 2024; Volume 2, pp. 19–44. [CrossRef]
47. Mondéjar-López, M.; García-Simarro, M.P.; Navarro-Simarro, P.; Gómez-Gómez, L.; Ahrazem, O.; Niza, E. A review on the encapsulation of "eco-friendly" compounds in natural polymer-based nanoparticles as next generation nano-agrochemicals for sustainable agriculture and crop management. *Int. J. Biol. Macromol.* **2024**, *280*, 136030. [CrossRef]
48. Hao, J.H.; Lv, S.S.; Bhattacharya, S.; Fu, J.G. Germination response of four alien congeneric *Amaranthus* species to environmental factors. *PLoS ONE* **2017**, *12*, e0170297. [CrossRef]
49. Singh, A.; Mahajan, G.; Chauhan, B.S. Germination ecology of wild mustard (*Sinapis arvensis*) and its implications for weed management. *Weed Sci.* **2022**, *70*, 103–111. [CrossRef]
50. Bana, R.S.; Kumar, V.; Sangwan, S.; Singh, T.; Kumari, A.; Dhanda, S.; Dawar, R.; Godara, S.; Singh, V. Seed germination ecology of *Chenopodium album* and *Chenopodium murale*. *Biology* **2022**, *11*, 1599. [CrossRef]
51. Loades, E.; Pérez, M.; Turečková, V.; Tarkowská, D.; Strnad, M.; Seville, A.; Nakabayashi, K.; Leubner-Metzger, G. Distinct hormonal and morphological control of dormancy and germination in *Chenopodium album* dimorphic seeds. *Front. Plant Sci.* **2023**, *14*, 1156794. [CrossRef]
52. Voegele, A.; Graeber, K.; Oracz, K.; Tarkowská, D.; Jacquemoud, D.; Tarkowská, V.; Urbanová, T.; Strnad, M.; Leubner-Metzger, G. Embryo growth, testa permeability, and endosperm weakening are major targets for the environmentally regulated inhibition of *Lepidium sativum* seed germination by myrigalone. *J. Exp. Bot.* **2012**, *63*, 5337–5350. [CrossRef]
53. Bachheti, A.; Sharma, A.; Bachheti, R.; Husen, A.; Pandey, D. Plant allelochemicals and their various applications. In *Co-Evolution of Secondary Metabolites*; Reference Series in Phytochemistry; Springer: Cham, Switzerland, 2020; pp. 441–465.
54. Pandharmise, P.; Tambe, A.N.; Kamble, S.; Tuwar, D.A. Preliminary phytochemical screening and HPTLC analysis of leaf extract of *Crotalaria juncea* from Vidarbha region, MS, India. *J. Maharaja Sayajirao Univ. Baroda* **2022**, *56*, 269–274.
55. Samajdar, S.; Mukherjee, S.; Das, P.P. Seed germination inhibitors: Molecular and phytochemical aspects. *Int. J. Appl. Pharm. Sci. Res.* **2018**, *3*, 12–23. [CrossRef]
56. Nikolova, M.; Yankova-Tsvetkova, E.; Stefanova, T.; Berkov, S. Exudate flavonoids of *Primula veris* leaves and their inhibitory activity on *Lolium perrene* seed germination. *Pap. Present. Proc. Bulg. Acad. Sci.* **2023**, *76*, 388–393. [CrossRef]
57. Torawane, S.; Mokat, D. Allelopathic potential of weed *Neanotis lancifolia* (Hook. f.) W.H. Lewis on seed germination and metabolism of mungbean and rice. *Allelopath. J.* **2021**, *52*, 277–290. [CrossRef]
58. Abdelmalik, A.M.; Alshahrani, T.S.; Alqarawi, A.A.; Ahmed, E.M. Allelopathic potential of *Nicotiana glauca* aqueous extract on seed germination and seedlings of *Acacia gerrardii*. *Diversity* **2024**, *16*, 26. [CrossRef]
59. Mahur, B.K.; Ahuja, A.; Singh, S.; Maji, P.K.; Rastogi, V.K. Different nanocellulose morphologies (cellulose nanofibers, nanocrystals and nanospheres) extracted from Sunn hemp (*Crotalaria Juncea*). *Int. J. Biol. Macromol.* **2023**, *253*, 126657. [CrossRef]
60. Lesiak, B.; Rangam, N.; Jiricek, P.; Gordeev, I.; Tóth, J.; Kövér, L.; Mohai, M.; Borowicz, P. Surface study of Fe_3O_4 nanoparticles functionalized with biocompatible adsorbed molecules. *Front. Chem.* **2019**, *7*, 642. [CrossRef]
61. Periakaruppan, R.; Kumar, T.S.; Vanathi, P.; Al-Awsi, G.R.L.; Al-Dayan, N.; Dhanasekaran, S. Phyto-synthesis and characterization of parthenium-mediated iron oxide nanoparticles and an evaluation of their antifungal and antioxidant activities and effect on seed germination. *Miner. Met. Mater. Soc.* **2023**, *75*, 5235–5242. [CrossRef]
62. Sainao, W.; Shi, Z.; Pang, H.; Feng, H. Alleviative effects of magnetic Fe_3O_4 nanoparticles on the physiological toxicity of 3-nitrophenol to rice (*Oryza sativa* L.) seedlings. *Open Life Sci.* **2022**, *17*, 626–640. [CrossRef]
63. Kornarzyński, K.; Sujak, A.; Czernel, G.; Wiącek, D. Effect of Fe_3O_4 nanoparticles on germination of seeds and concentration of elements in *Helianthus annuus* L. under constant magnetic field. *Sci. Rep.* **2020**, *10*, 8068.
64. Serpoush, M.; Kiyasatfar, M.; Ojaghi, J. Impact of Fe_3O_4 nanoparticles on wheat and barley seeds germination and early growth. *Mater. Today* **2022**, *65*, 2915–2919. [CrossRef]
65. Das, C.K.; Srivastava, G.; Dubey, A.; Verma, S.; Saxena, M.; Roy, M.; Sethy, N.K.; Bhargava, K.; Singh, S.K.; Sarkar, S.; et al. The seed stimulant effect of nano iron pyrite is compromised by nano cerium oxide: Regulation by the trace ionic species generated in the aqueous suspension of iron pyrite. *RSC Adv.* **2016**, *6*, 67029–67038. [CrossRef]
66. Gupta, N.; Singh, P.M.; Sagar, V.; Pandya, A.; Chinnappa, M.; Kumar, R.; Bahadur, A. Seed priming with ZnO and Fe_3O_4 nanoparticles alleviate the lead toxicity in *Basella alba* L. through reduced lead uptake and regulation of ROS. *Plants* **2022**, *11*, 2227. [CrossRef] [PubMed]
67. Alkhatib, R.; Alkhatib, B.; Abdo, N. Effect of Fe_3O_4 nanoparticles on seed germination in tobacco. *Environ. Sci. Pollut.* **2021**, *28*, 53568–53577. [CrossRef] [PubMed]

68. Khan, S.; Akhtar, N.; Rehman, S.U.; Shujah, S.; Rha, E.S.; Jamil, M. Biosynthesized iron oxide nanoparticles (Fe_3O_4 NPs) mitigate arsenic toxicity in rice seedlings. *Toxics* **2021**, *9*, 2. [CrossRef]
69. Xu, P.; Zeng, G.M.; Huang, D.L.; Feng, C.L.; Hu, S.; Zhao, M.H.; Lai, C.; Wei, Z.; Huang, C.; Xie, G.X.; et al. Use of iron oxide nanomaterials in wastewater treatment: A review. *Sci. Total Environ.* **2012**, *424*, 1–10. [CrossRef]